BÁNKI KÖZLEMÉNYEK
2. ÉVFOLYAM 2. SZÁM

Comparison of creep behavior for lead free solders Sn-3.5Ag, SAC305 and SAC387

Vargas C. Ramiro S. *, Gonda Viktor **
*Doctoral School on Materials Sciences and Technologies, Óbuda University,
1034 Bécsi út 96/b, Budapest, Hungary
** Bánki Faculty of Mechanical and Safety Engineering, Óbuda University,
1081 Népszínház u. 8, Budapest, Hungary
vargas.ramiro@phd.uni-obuda.hu, gonda.viktor@bgk.uni-obuda.hu

***Abstract* — Numerous lead-free solder compositions were developed recently to substitute the conventional lead-tin solder due to its environmental hazards. As an example, lead-free solders with tin-silver-copper (SAC) compositions are frequently used with various weigh percentage of the alloying elements. Beside the electronic properties of these solders, the mechanical behavior is of great interest, due to the time dependent nature arising from these low melting point materials operating at thermal-mechanical loads. In this paper, the thermal-mechanical creep behavior is analyzed for three lead-free solders of Sn-3.5Ag; SAC305 and SAC387. A simple structural configuration of an electronic package containing a solder joint is modeled in finite elements, where the applied load was thermal cycling. The Anand material model was employed for the creep behavior of the solder. Stress and strain analyses of the structural behavior was performed and compared for the tree different lead-free solders. Results are presented for the mechanical response of the different compositions.**

***Keywords*:** Lead-free solder, creep, finite element analysis.

1 INTRODUCTION

The first patents and concepts of the printed circuit board (PCB) where introduced by Charles L. in 1925 [1]. Basically, it consisted of a copper layer in the shape of a path that interconnected electronic components. This concept replaced the traditional wiring process in circuit manufacturing. Initially, Integrated Circuits (IC) and electronic components had external lead pins attached to the encapsulated circuit. After mounting the electronic components over the PCB, a joining material was needed to fix the circuit to the board. This material known as solder is a fusible alloy with a low melting temperature and commonly with eutectic chemical composition.

Due to downscaling, smaller electronic components where developed, and new surface mounting technologies were released as well. The Flip Chip (FC) assembly was found to one of the most advantageous in terms of space optimization.

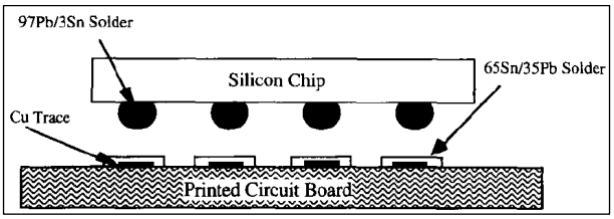

Figure 1. Flip Chip placement operation [2].

Figure 1 illustrates how the traditional external lead pins attached to the electronic components were replaced by metalized pads.

1.1 Solder materials

The solder material is responsible for the mechanical and electrical joining between the copper path and the electronic component. Moreover, the current that flows through the solder during the operation leads to cycling thermal load. Table 1 details some of the most common environmental temperature ranges according to the application of electronic packaging.

Table 1. Thermal environments for solder joints in a variety of electronic packages [3].

Use conditions	Thermal excursion (°C)
Consumer electronics	0 to 60
Computers	15 to 60
Telecommunications	– 40 to 85
Commercial aircraft	– 55 to 95
Military aircraft	– 55 to 125
Space	– 40 to 85
Automotive – Passenger compartment	– 55 to 65
Automotive – Under the hood	– 55 to 150

Basically, the solder material interacts with copper and ceramics under specific thermal stress and current flow. This combination of loads certainly causes a fatigue load over the joint which eventually may produce residual deformation, and eventually fracture. To prevent such failures, epoxy encapsulation may be used to prolong the thermal fatigue up to 200 times than the non-encapsulated joints [4].

For over 50 years, the eutectic tin-lead (SnPb) solder was used due to its unique combination of outstanding properties and reliability. Although lead is economically suitable, it was found to be hazardous for humans. Lead may interfere with the reproductive and cardiovascular systems amongst others [5]. Therefore, in 2002 the European Parliament released the Restriction of Hazardous Substances Directive (RoHS) regarding the usage restriction of lead in electrical and electronic equipment [6]. This regulation document was upgraded in 2011 [7] with more specific percentages per weight and some exceptions. RoHS did not only affect European industries, but also the market from China, Japan, South Korea, Tukey and the United States of America. As the deadline to apply such restriction in 2006 was closer, thin-silver-copper (SnAgCu) or simply called SAC solders was discovered to be one of

the most promising replacement for the eutectic SnPb solder [8]. Philips presented their first results testing SAC405 (Ag 4%; Cu 0.5%) in 2004. They faced some issues due to solder pre-heat time that damaged the plastic housing of electro/magnetic components. Furthermore, it was proposed, that the design rule changes regarding round pad dimensions [9]. In short, any solder material further discovered must meet precise characteristics for a high performance and long lasting of electronic devices.

1.2 Creep

Creep is defined as the time–dependent plastic strain at constant stress above the melting temperature (T_m) [10]. Creep comprises three stages: primary, secondary and tertiary (see Figure 2, [10]). Along the primary stage (strain–hardening), the strain rate decreases, as hardening of the metal becomes more difficult. During the secondary stage, the strain rate is constant, this is usually called steady–state (SS) creep rate ($\dot{\varepsilon}_{SS}$). Finally, in the tertiary stage the strain rate rises exponentially and eventually leads to a material fracture [11].

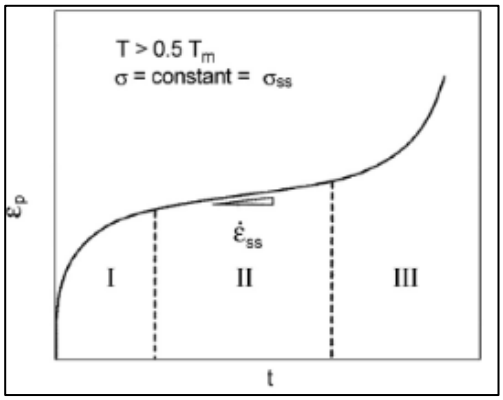

Figure 2. Constant true stress and constant strain rate creep behavior.

1.2.1 The Power Law model

Creep during the secondary state exhibits a direct proportion to temperature and stress. Thus, basic power law (also known as Norton's Law) can be expressed as follows:

$$\dot{\varepsilon}_{ss} = B\sigma^n \tag{1}$$

where B is a temperature-dependent material parameter and n is the stress exponent. Through mathematical modelling, Ahmad et al. [12] expanded (1) into $\dot{\varepsilon}^c = A\sigma^n T^p$ where A and p are both characteristic constants of the material. Additionally, Brown and Ashby [13] suggests a strong logarithmic relation between Dorn constant (A) and the exponent n. Parameter n from (1) is 4 to 5 for pure metals (for that reason called "five" power law). It is also associated with dislocation creep (n = 4-5) and purely diffusive creep (n = 1) [14]. From power law, multiple equations have been derived using several parameters that belong to the material of interest.

1.2.2 Diffusive creep

In terms of microstructure, lattice plane contains at least three nonlinear lattice points. Diffusional creep involves changes in lattice planes that consequently affect vacancies [15]. According to the research done by Mesarovic [16], depending on the temperature and stress level, several micro-mechanisms of creep can be distinguished (see Table 2).

Table 2. Micro-mechanism of Creep [10-13].

Creep	Description
Nabarro–Herring [10–12] 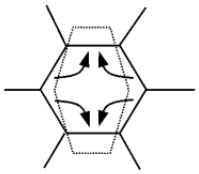	Diffusion of vacancies through the crystalline lattice and complementary diffusion of atoms through the vacancy–atom exchange mechanism, leads to the creation of new lattice layers on some boundaries and disappearance of lattice layers on other boundaries.
Coble [12, 13] 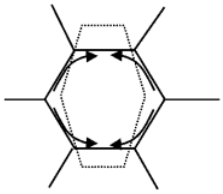	Diffusion of vacancies/atoms along grain boundaries with the same outcome: lattice growth/disappearance.
Dislocation	Vacancy diffusion enables dislocation climb and glide.

1.2.3 Harper-Dorn Creep

In 1957 Harper and Dorn [21] suggested a new model for materials subjected to low-stresses. Harper and Dorn found that the steady-state creep rate increased linearly with the applied stress. After several experiments on aluminum, equation (2) was proposed [22].

Harper-Dorn formal model:

$$\dot{\varepsilon}_{ss} = A_{HD}\left(\frac{D_1 Gb}{kT}\right)\left(\frac{\sigma}{G}\right)^1 \tag{2}$$

where D_1 is the diffusion coefficient for lattice self-diffusion, G is the shear modulus, b is the Burger's vector, k is Boltzmann's constant, T is the absolute temperature, σ is the applied stress, and A_{HD} is a dimensionless constant of the order of 10-11. The early results of Harper-Dorn model was lately confirmed with test in pure aluminum by Barrett et al. [23] and Mohamed et al. [24].

2 METHODOLOGY

The following case study compares the equivalent creep strain and stress of three lead free solders with the eutectic thin-lead solder. The modelled 2-D cross section shown in Figure 3 comprises part of a FC assembly where the housing material of the electronic component is assumed to be ceramic as suggested by MSC software's User Guide [25].

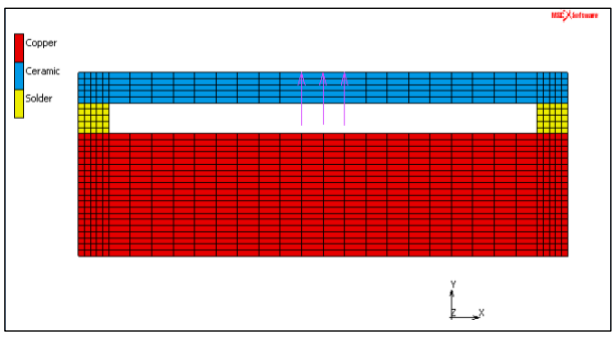

Figure 3. Structural setup and materials description of the sample.

The software package used to run the simulations was MARC Mentat, where within the viscoplasticity properties, there are two options to process creep analysis: Power Law and Anand Model. Since Anand model implies more parameters, this method was chosen to have more accurate results.

2.1 Anand Model

In 1982 Anand [26] proposed two evolution equations from the flow equation (3) based on earlier theories suggested by Lee and Zaverl [27]. The main purpose of this research was a better analysis deformation of metals at elevated temperatures above $0.5{\times}T_m$ (melting temperature). However, in 1985, after considering the second tensor (4) as another parameter which characterize the plastic state of a material, (5) and (6) where finally proposed [28].

Flow equation:

$$\dot{\varepsilon_p} = A \cdot \exp\left(-\frac{Q}{RT}\right)\left(\sinh\left(\xi\frac{\sigma}{s}\right)\right)^{1/m} \tag{3}$$

where,

A: Pre-exponential factor.
Q: Activation energy.
R: Boltzmann constant.
ξ: Multiplier of stress.
s: Deformation resistance.
m: Strain rate sensitivity of stress.

Second tensor equation:

$$\mathrm{B} = 1 - \frac{s}{s^*} \tag{4}$$

where,

s^*: Saturation resistance.

Evolution equations:

$$\dot{s} = \{h_0|\mathrm{B}|^a \mathrm{sgn}(\mathrm{B})\}\dot{\varepsilon_p} \tag{5}$$

$$s^* = \hat{s}\left(\frac{\dot{\varepsilon_p}}{A}\exp\left(\frac{Q}{RT}\right)\right)^n \tag{6}$$

where,

h_0: Hardening constant.
a: Strain rate sensitivity of hardening.
$\hat{s}$: Deformation resistance saturation coefficient.
n: Strain rate sensitivity of saturation.

To summarize, Anand model involves nine material parameters: A, Q, ξ, m, h_0, $\hat{s}$, n, m and s_0, which is the initial value of the deformation resistance needed to determine the evolution of the deformation resistance. All those values can be determined following Brown's procedure [29] who suggest at least two sets of three strain rate jump tests performed at different temperatures. However, this research takes all Anand's values from characterizations and previous studies.

2.2 Material Properties

As this research describes creep behavior using Anand Model, viscoplastic properties must be established. Table 3 details the parameters for the eutectic SnPb solder as well as for the three lead-free solders of interest. It should be mentioned that most of the authors do not tabulate the activation energy, but they were computed using the Boltzmann constant.

Table 3 enumerates the thermomechanical properties of the materials graphically described in Figure 3. Before entering the values to the simulation software, all units must work in the same metric prefix in terms of stress (MPa).

Table 3. Material parameters for Anand model.

Description	**Sn3.5Ag**[30]	**SAC 305**[31]	**SAC 387**[32]	**SnPb**[25]
s_0 (MPa)	0.65	21	37.1	56.33
A (s^{-1})	344.716	3 501	65.92	$1.49{\cdot}10^7$
ξ	3	4	8	11
m	0.143	0.25	0.346	0.303
h_0 (MPa)	23 241	180 000	86 442.8	2 640.75
$\hat{s}$ (MPa)	26	30.2	80.8	80.42
n	0.0447	0.01	0.0002	0.0231
a	1.46	1.78	1.29	1.34
Q ($\mathrm{J{\cdot}mol^{-1}}$)	54 364	77 490.78	55 307.8	90 040

Additionally, Table 4 not only describes thermomechanical properties needed for the Anand modelling, but also the melting temperature of each solder material. Indeed, the eutectic SnPb clearly shows the lowest temperature amongst the solder materials.

Table 4. Thermomechanical properties.

Material	**T range (°C)**	***E* (GPa)**	***ν***	***α* (ppm/°C)**	***T_m* (°C)**
Sn3.5Ag [33]	20 – 150	48 – 25	0.40	20.2 – 21.7	221
SAC 305 [34]	25 – 125	90 – 38	0.42	16 – 22.4	217
SAC 387 [35]	20 – 100	46 – 35	0.40	17.6	217
SnPb [36]	25 – 125	22 – 12	0.40	21	183
Cu [4, 9]	–	1.3	0.34	17	1084
Ceramic [25]	–	0.375	0.22	5.36	–

2.3 Load case

The center of the ceramic part (see Figure 4) was subjected to a vibration load with a minimum displacement of 0.5 (mm) in the vertical axis *(y)*. Figure 5 describes the load which consists of a sinusoidal oscillation of four cycles running for one-hundred and twenty seconds (120 s).

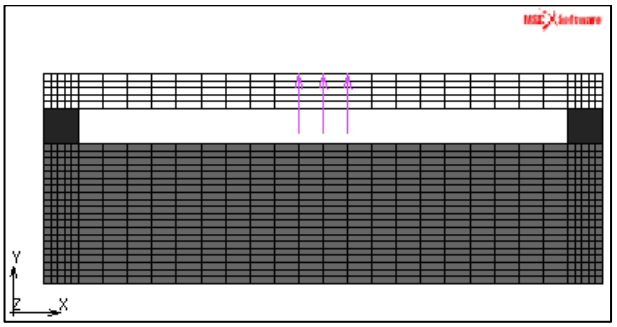

Figure 4. Vibration load's location.

Simultaneously, a thermal load which changes the temperature of the entire sample from 0 to 125 (°C) is also applied describing two cycles (see Figure 6).

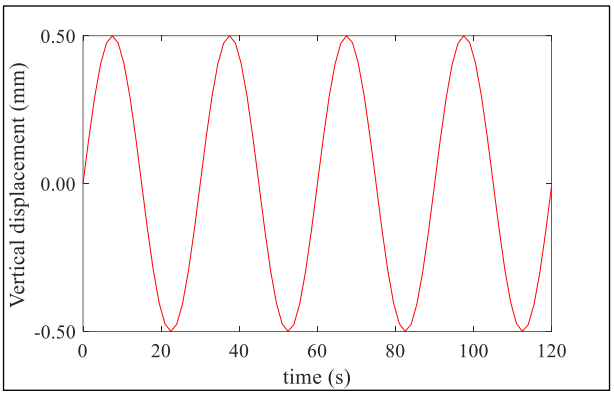

Figure 5. Sinusoidal Structural Loading vs Time.

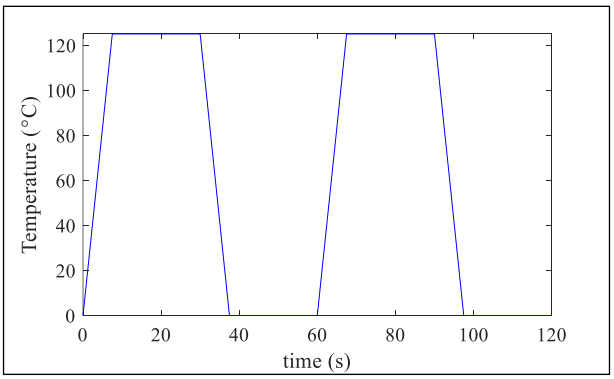

Figure 6. Thermal load Temperature vs Time.

2.4 Boundary conditions

As the vibration load case mainly result in displacement, the bottom part of the copper layer must be totally fixed. Thus, restriction regarding displacement and rotation in all the three axes where applied to the bottom part of the sample (see Figure 7).

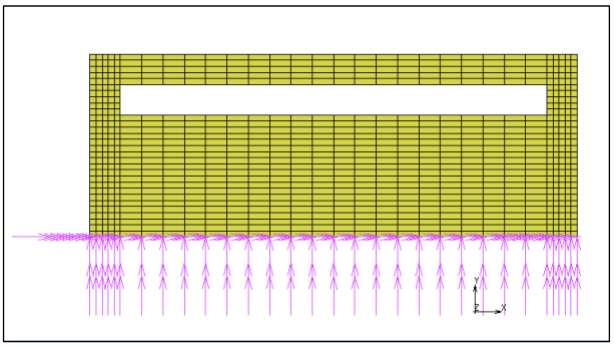

Figure 7. Bottom constraints.

The cross section graphically described in Figure 3 is only part of an entire FC assembly. However, it could be either in the side or in the middle.

To obtain the critical values, it was assumed to be in the middle. Thus, displacement restriction in the horizontal axis *(x)* was applied to both side parts of the sample (see Figure 8).

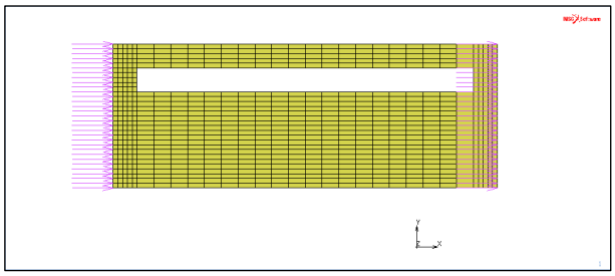

Figure 8. Periodical boundary condition.

2.5 Point of analysis

As the main interest of this research is to determine the creep behavior of the solders, a middle inner point was selected to collect the data (see Figure 9). Basically, equivalent creep strain, total equivalent creep strain and total equivalent stress data were collected from the before described node.

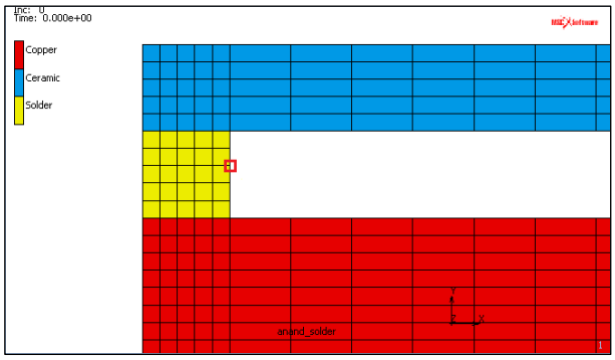

Figure 9. Point of analysis.

3 RESULTS AND DISCUSSION

Although the load case remained stable for all the simulations and only viscoplastic parameters were changed, job parameters were set automatically by the program. When job parameters were adjusted to obtain 400 samples per node, the software was not able to run the simulation. This resulted in different data sets between 50 to 130 samples per node as summarized in Table 5.

Table 5. Samples per material.

Material	Number of samples
Sn3.5Ag	127
SAC 305	116
SAC 387	91
SnPb	54

After several simulations, Figure 10 reveals that the equivalent creep strain describes four cycles like the vibration load. However, only the first five semi-cycles present a slight constant difference between solders. For instance, during the sixth semi-cycle of the SnPb a crest was expected. Likewise, during the seventh semi-cycle, the Sn3.5Ag crest is not as high as the previous crest of the same solder.

Furthermore, Figure 11 shows the evolution of the total equivalent creep strain where after 120 sec., final values were as follow: SnPb 0.23(s^{-1}), Sn3.5Ag 0.18(s^{-1}), SAC305 0.12(s^{-1}) and SAC387 0.14(s^{-1}). Evidently, SAC305 shows the minimum total equivalent creep strain, with nearly 48% less than the SnPb value. However, the three lead free

solders still describe a lesser total equivalent creep strain as compared to SnPb.

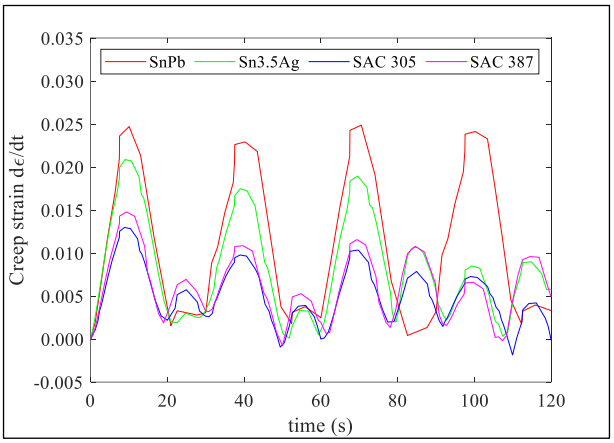

Figure 10. Equivalent Creep Strain - Comparison.

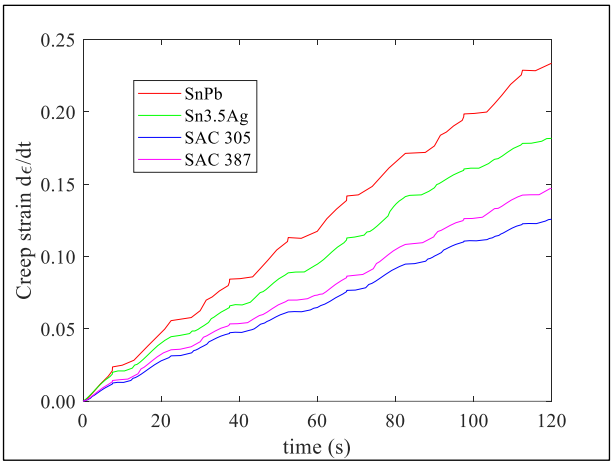

Figure 11. Total Equivalent Creep Strain - Comparison

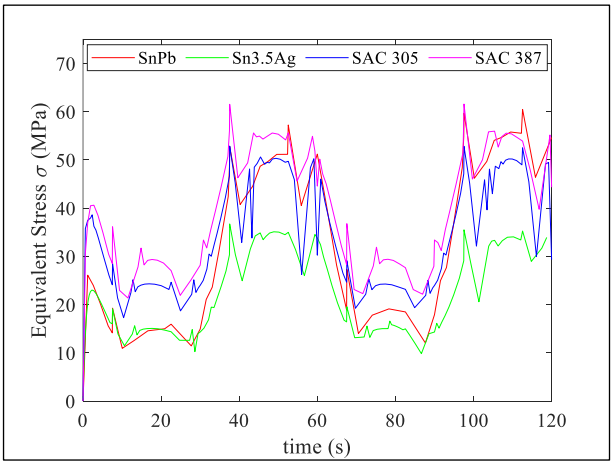

Figure 12. Total Equivalent Stress.

Unlike creep strain curves, Figure 12 describes only two cycles of oscillating stress. As the temperature increases the stress decreases in contrast with Figure 6. Moreover, Sn3.5Ag and SAC387 curves present the minimum and maximum values respectively along most of the graph.

Table 6 summarizes the average and maximum value of the equivalent creep strain as well as from the total equivalent stress. Certainly, SAC305 shows the minimum average creep strain (4.8×10^{-3}) whereas SnPb shows the maximum average value (12.1×10^{-3}). On the other hand, regarding total equivalent stress, Sn3.5Ag shows the minimum average value (19.70 MPa) whereas SAC 387 shows the maximum average value (39.38 MPa).

Table 6. Main values of equivalent creep and stress.

		SnPb	Sn3.5Ag	SAC305	SAC387
Creep ($\times10^{-3}$)	Max	24.9	20.9	13.0	14.8
	Av	12.1	7.03	4.80	5.64
Stress (MPa)	Max	60.46	36.72	52.87	61.57
	Av	33.57	19.70	34.66	39.98

4 Conclusions

Creep strain rate is a complex time–dependent mechanical behavior that must be considered for a proper constant functioning of electronic boards. The eutectic solder material, SnPb has a low melting temperature which is favorable for manufacturing electronic PCB and has been proven to be long lasting. However, new lead-free compositions are replacing the eutectic SnPb solder due to new international regulations. The yield of unleaded solders under thermomechanical loads must be discussed to guarantee a correct long–lasting efficient work and then replace the leaded solders.

Through a simulation, a sample was subjected to cyclic mechanical and thermal loads. On one hand the thermal load presented two entire cycles whereas, the vibration load oscillated four times.

From the equivalent creep strain comparison, it is evident that the mechanical load governs the creep behavior rather than the thermal load. From the results in terms of total equivalent creep strain, unleaded solders clearly present a favorable value with nearly fifty percent less than the eutectic solder. Certainly, SAC305 and SAC387 seem to have a high similarity regarding thermomechanical properties. However, the total equivalent creep strain of SAC305 is leaser than SAC387 with a final total equivalent creep strain of 0.12 (s^{-1}) and 0.14 (s^{-1}) respectively.

On the other hand, the total equivalent stress graph correlates the thermal load displaying two cycles. Regarding the total equivalent stress, Sn3.5Ag presents the minimum values, whereas SAC 387 presents the maximum. Indeed, the curve described by the eutectic solder is not highly different from the SAC solders. Additionally, the average stress of the eutectic solder is slightly lesser than the SAC305 and SAC387.

To sum up, lead free solder materials manifest better creep strain rates under thermomechanical loads in comparison with eutectic SnPb solder. Yet, further analysis should be carried out to determine which one presents a better yield in another time dependent variable and still present an acceptable creep behavior.

References

[1] D. Charles, “Electrical apparatus and method of manufacturing the same,” 01-Dec-1925.

[2] G. O’Malley, J. Giesler, and S. Machuga, “The importance of material selection for flip chip on board assemblies,” *IEEE Trans. Components, Packag. Manuf. Technol. Part B*, vol. 17, no. 3, pp. 248–255, 1994.

[3] D. R. Frear, S. N. Burchett, H. S. Morgan, and J. H. Lau, Mechanics of solder alloy interconnects. Springer Science & Business Media, 1994.

[4] Y. Tsukada, H. Nishimura, M. Sakane, and M. Ohnami, "Fatigue Life Analysis of Solder Joints in Flip Chip Bonding," J. Electron. Packag., vol. 122, no. 3, p. 207, 2000.

[5] D. S. Herman, M. Geraldine, C. C. Scott, and T. Venkatesh, "Health hazards by lead exposure: evaluation using ASV and XRF," Toxicol. Ind. Health, vol. 22, no. 6, pp. 249–254, Jul. 2006.

[6] EUROPEAN PARLIAMENT; THE COUNCIL OF THE EUROPEAN UNION, "Directive 2002/95/EC of the European Parliament and of the Council of 27 January 2003 on the restriction of the use of certain hazardous substances in electrical and electronic equipment.," Official Journal of the European Union, 2003. .

[7] EUROPEAN PARLIAMENT; THE COUNCIL OF THE EUROPEAN UNION, "DIRECTIVE 2011/65/EU OF THE EUROPEAN PARLIAMENT AND OF THE COUNCIL of 8 June 2011 on the restriction of the use of certain hazardous substances in electrical and electronic equipment (recast)," Official Journal of the European Union, 2011. .

[8] S. Cheng, C. M. Huang, and M. Pecht, "A review of lead-free solders for electronics applications," Microelectron. Reliab., vol. 75, pp. 77–95, 2017.

[9] S. Yue, "Philips our experience in the introduction of leadfree soldering," in 2004 International IEEE Conference on the Asian Green Electronics (AGEC). Proceedings of, pp. 18–25.

[10] M. E. Kassner, Fundamentals of Creep in Metals and Alloys. Elsevier, 2015.

[11] G. Dieter, "Mechanical Metallurgy." p. 615, 1961.

[12] M. I. M. Ahmad, J. L. Curiel Sosa, and J. A. Rongong, "Characterisation of creep behaviour using the power law model in copper alloy," J. Mech. Eng. Sci., vol. 11, no. 1, pp. 2503–2510, Mar. 2017.

[13] A. M. Brown and M. F. Ashby, "On the power-law creep equation," Scr. Metall., vol. 14, no. 12, pp. 1297–1302, Dec. 1980.

[14] S. Spigarelli, "Creep of Aluminium and Aluminium Alloys," Talat, p. 26, 1999.

[15] C. Kittel, Introduction to solid state physics, vol. 8. Wiley New York, 1976.

[16] S. D. Mesarovic, "Lattice continuum and diffusional creep," Proc. R. Soc. A Math. Phys. Eng. Sci., vol. 472, no. 2188, 2016.

[17] F. R. N. Nabarro, "Report of a Conference on the Strength of Solids," Phys. Soc. London, vol. 75, 1948.

[18] C. Herring, "Diffusional viscosity of a polycrystalline solid," J. Appl. Phys., vol. 21, no. 5, pp. 437–445, 1950.

[19] G. FANTOZZI, J. CHEVALIER, C. OLAGNON, and J. L. CHERMANT, "Creep of Ceramic Matrix Composites," in Comprehensive Composite Materials, Elsevier, 2000, pp. 115–162.

[20] R. L. Coble, "A model for boundary diffusion controlled creep in polycrystalline materials," J. Appl. Phys., vol. 34, no. 6, pp. 1679–1682, 1963.

[21] J. Harper and J. E. Dorn, "Viscous creep of aluminum near its melting temperature," Acta Metall., vol. 5, no. 11, pp. 654–665, 1957.

[22] P. Yavari, D. A. Miller, and T. G. Langdon, "An investigation of harper-dorn creep—I. Mechanical and microstructural characteristics," Acta Metall., vol. 30, no. 4, pp. 871–879, Apr. 1982.

[23] C. R. Barrett, E. C. Muehleisen, and W. D. Nix, "High temperature-low stress creep of Al and Al+ 0.5% Fe," *Mater. Sci. Eng.*, vol. 10, pp. 33–42, 1972.

[24] F. A. Mohamed, K. L. Murty, and J. W. Morris, "Harper-dorn creep in al, pb, and sn," Metall. Trans., vol. 4, no. 4, pp. 935–940, 1973.

[25] MSC Software Corporation, Theory and User Information. 2018.

[26] L. Anand, "Constitutive Equations for the Rate-Dependent Deformation of Metals at Elevated Temperatures," J. Eng. Mater. Technol., vol. 104, no. 1, p. 12, 1982.

[27] D. Lee and F. Zaverl Jr, "A generalized strain rate dependent constitutive equation for anisotropic metals," Acta Metall., vol. 26, no. 11, pp. 1771–1780, 1978.

[28] L. Anand, "Constitutive equations for hot-working of metals," Int. J. Plast., vol. 1, no. 3, pp. 213–231, 1985.

[29] S. B. Brown, "An Internal Variable Constitutive Model for the Thixotropic Behavior of Metal Semi-Solid Slurries," Materials Science Seminar on Intelligent Processing of Materials, vol. 5. pp. 95–130, 1989.

[30] N. Bai, X. Chen, and H. Gao, "Simulation of uniaxial tensile properties for lead-free solders with modified Anand model," Mater. Des., vol. 30, no. 1, pp. 122–128, 2009.

[31] M. Basit, M. Motalab, J. C. Suhling, and P. Lall, "Viscoplastic Constitutive Model for Lead-Free Solder Including Effects of Silver Content, Solidification Profile, and Severe Aging," in Volume 2: Advanced Electronics and Photonics, Packaging Materials and Processing; Advanced Electronics and Photonics: Packaging, Interconnect and Reliability; Fundamentals of Thermal and Fluid Transport in Nano, Micro, and Mini Scales, 2015, p. V002T01A002.

[32] J. H. L. Pang, Lead Free Solder, vol. 9781461404. New York, NY: Springer New York, 2012.

[33] National Institute of Standards and Technology (NIST), "Sn-Ag Properties and Creep Data." [Online]. Available: https://www.metallurgy.nist.gov/solder/clech/Sn-Ag_Other.htm#Poisson.

[34] T. T. Nguyen, D. Yu, and S. B. Park, "Characterizing the mechanical properties of actual SAC105, SAC305, and SAC405 solder joints by digital image correlation," J. Electron. Mater., vol. 40, no. 6, pp. 1409–1415, 2011.

[35] National Institute of Standards and Technology (NIST), "Sn-Ag-Cu Properties and Creep Data." [Online]. Available: https://www.metallurgy.nist.gov/solder/clech/Sn-Ag-Cu_Other.htm.

[36] Q. J. Yang, X. Q. Shi, Z. P. Wang, and Z. F. Shi, "Finite-element analysis of a PBGA assembly under isothermal/mechanical twisting loading," Finite Elem. Anal. Des., vol. 39, no. 9, pp. 819–833, 2003.

[37] J. R. Davis, "ASM specialty handbook," *Stainl. Steel*, vol. 10, 1994.